JOURNAL OF GUIDANCE, CONTROL, AND DYNAMICS
Vol. 15, No. 5, September-October 1992

Linear Quadratic Servo Control of a Reusable Rocket Engine

Jeffrey L. Musgrave*
NASA Lewis Research Center, Cleveland, Ohio 44135

This work develops a new design method for the servo compensator in the frequency domain using singular value inequalities and applies the method to a reusable rocket engine. The servo compensator allows command following with set point control that is necessary for engine throttling during downthrust maneuvers. A Kalman filter reconstructs the engine state vector and loop transfer recovery recovers the required degree of robustness while maintaining satisfactory rejection of sensor noise from the command error. The approach is applied to the design of a linear controller for a reusable rocket engine satisfying performance constraints in the frequency domain. Simulation results demonstrate the performance of the linear control design on a nonlinear rocket engine model over power levels typical of mainstage operation.

Introduction

AN intelligent control system for reusable rocket engines has been proposed[1] for the purposes of widening the range of operation, enhancing overall engine performance, and reducing the amount of required maintenance. This work develops a new control design method in the frequency domain for the servo compensator,[2] which meets the various requirements of a controller for an intelligent control system and applies the method to the Space Shuttle main engine.

The use of the linear quadratic regulator for the design of a command following controller was first introduced by Athans.[3] Davison and Goldenberg[2] used state augmentation in a similar manner to synthesize the robust servo compensator possessing certain degrees of robustness to variations in the plant model based on the availability of outputs for measurement. Their method relied primarily on augmenting the state vector of the plant with an internal model of the plant disturbances and reference commands, resulting in a multivariable compensator with a stabilizing loop and a feed-forward loop. Davison[4] proposed a technique for constructing the gains of the servo compensator for the case where the plant model is unknown. Wang and Munro[5] extended earlier results by demonstrating how the servo compensator could be used with linear quadratic regulator theory to synthesize controller gains for both step and ramp disturbances and input commands.

A majority of the analysis procedures for determining the degree of robustness in a closed-loop control system are typically specified in the frequency domain using singular values of the sensitivity

$$S(s) = [I + G(s)K(s)]^{-1}$$

and complementary sensitivity

$$T(s) = G(s)K(s)[I + G(s)K(s)]^{-1}$$

functions as a measure of worst case behavior.[6,7] The linear quadratic Gaussian/loop transfer recovery (LQG/LTR) methodology[8] employs these ideas directly in the design and analysis of a dynamic compensator using loop shaping ideas in the frequency domain on transfer functions created by breaking loops at physical points designated by XX in Fig. 1. The results presented here extend the basic control structure of Davison and Goldenberg into a new frequency-domain design methodology using singular value inequalities, loop transfer recovery, and optimal control.

This paper presents a new method for designing linear multivariable controllers for an intelligent control system for reusable rocket engines. A servomechanism approach allows set point control with command following. The design method is presented along with an analysis of the performance and robustness characteristics. Estimator design is performed in the framework of the Kalman filter formalism, with emphasis on using a sensor set different from the commanded variables. Loop transfer recovery modifies the nominal plant noise intensities to obtain the desired degree of robustness to uncertainty reflected at the plant input. An example demonstrates the technique in the design of a controller for the Space Shuttle main engine.

Servo Compensator with LTR

Consider a proper linear time-invariant system written in state space form as

$$\begin{aligned} \dot{x}(t) &= Ax(t) + Bu(t) + \zeta(t) \\ y(t) &= Cx(t) \\ z(t) &= Hx(t) + \Gamma\eta(t) \end{aligned} \tag{1}$$

where $x \in \Re^n$, $u \in R^m$, $z \in R^m$, and $y \in R^r$, with matrices A, B, C, H, and Γ all of appropriate dimensions with $m \geq r$. Additionally, $\zeta(t)$ and $\eta(t)$ are zero mean vector random processes with normal distributions with intensities $Q_p = Q_p^T \in \Re^{n\times n}$, $Q_p \geq 0$, $R_s = R_s^T \in \Re^{m\times m}$, and $R_s > 0$, respectively. The expression $y(t)$ and $r(t)$ represent commanded quantities and reference commands, respectively. The measurements $z(t)$ are used for state reconstruction via the Kalman filter. A control law of the form

$$u(t) = -K_{sp}x(t) - K_i\int_0^t e(\tau)\,d\tau \tag{2}$$

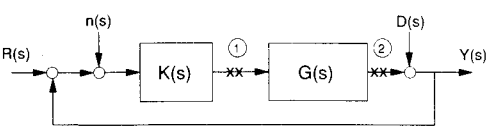

Fig. 1 Typical feedback setup.

Received May 1, 1991; revision received Oct. 31, 1991; accepted for publication Nov. 12, 1991.

*Controls Research Engineer, Advanced Control Technology Branch, MS 77-1.

is desired, where $e(t) = r(t) - y(t)$, $K_{sp} \in \Re^{m \times n}$, and $K_i \in \Re^{m \times r}$. The problem is well posed if the pair (A, B) is stabilizable, if (H, A) and (C, A) are detectable, and if transmission zeros of $\{A, B, C\}$ do not appear at the origin.[2]

K_{sp} and K_i are determined by augmenting the state with

$$e_a(t) = \int_0^t [y(\tau) - r(\tau)]\, d\tau \tag{3}$$

giving

$$\frac{d}{dt}\begin{bmatrix} x(t) \\ e_a(t) \end{bmatrix} = \begin{bmatrix} A & 0 \\ C & 0 \end{bmatrix}\begin{bmatrix} x(t) \\ e_a(t) \end{bmatrix} + \begin{bmatrix} B \\ 0 \end{bmatrix} u(t) \tag{4}$$

when $r(t)$ is zero. The synthesis problem may be solved by minimizing a standard quadratic cost function

$$\frac{1}{2}\int_0^\infty [x(\tau)\ e_a(\tau)] Q_a \begin{bmatrix} x(\tau) \\ e_a(\tau) \end{bmatrix} + u(\tau)^T R u(\tau)\, d\tau \tag{5}$$

where $R = R^T > 0$ and Q_a is typically taken to be

$$Q_a = \begin{bmatrix} 0 & 0 \\ 0 & Q \end{bmatrix} \tag{6}$$

with $Q = Q^T \in \Re^{r \times r}$ and $Q^T > 0$. The detectability of (C, A) is required due to the special structure of the weighting matrix Q_a for the augmented system. The linear state feedback control satisfying this minimization problem can be obtained from the solution P of an algebraic Riccati equation (ARE) such that

$$[K_{sp}\ K_i] = R^{-1}\begin{bmatrix} B \\ 0 \end{bmatrix}^T P \tag{7}$$

The design reduces to the selection of the matrices Q and R satisfying performance and robustness constraints prescribed for the closed-loop system.

Servo Compensator Design

To design a controller with good command following and robustness to modeling errors and plant disturbances, the singular values of two different transfer functions must be designed simultaneously. Figure 2 shows the servo compensator configuration with full state feedback. The design of a controller with good command following properties requires $R(s) = Y(s)$ over the range of frequencies contained in typical inputs. For design purposes, $Y(s)$ may be written as

$$Y(s) = [I + C\Phi B(I + K_{sp}\Phi B)^{-1} G_y(s)]^{-1} \times C\Phi B(I + K_{sp}\Phi B)^{-1} G_y(s) R(s) \tag{8}$$

where $R(s) \in C^m$, $\Phi = (sI - A)^{-1}$, and $G_y(s) = K_i(sI)^{-1}$. Good command following requires

$$\underline{\sigma}\,[C\Phi B(I + K_{sp}\Phi B)^{-1} G_y(s)] \gg 1 \tag{9}$$

where $\underline{\sigma}(\ )$ represents the minimum singular value that follows immediately from the properties of singular values.[8] The transfer function appearing in Eq. (9) corresponds to breaking the error loop at the XX shown at point 2 in Fig. 2 and synthesizing the open-loop transfer function from $E'(s)$ to $E''(s)$ with $R(s) = 0$. The singular values may be altered directly by modifying the weights in the solution of the ARE until the minimum singular value has a satisfactory gain over all frequencies of interest.

The controller should also possess a certain degree of robustness to low-frequency modeling errors as indicated in Fig. 2 by $D(s)$. In particular, the effect of $D(s)$ on $E(s)$ should be made as small as possible. To determine the requirement explicitly, $E(s)$ may be written as

$$E(s) = -[I + C\Phi B(I + K_{sp}\Phi B)^{-1} G_y(s)]^{-1} D(s) \tag{10}$$

which shows that the condition specified in Eq. (9) for good command following is sufficient to guarantee disturbance rejection resulting from low-frequency modeling errors.

The final issue in the servo design involves minimizing the impact of modeling errors reflected at the plant input by considering the physical point at 1 in Fig. 2. Additionally, the effect of any sensor noise on the command channel can be included with "modeling errors" as with any noise on the channel connecting the controller to the plant. The control input equation may be written as

$$U(s) = -K_{sp}X(s) + G_y(s)[R(s) - Y(s)] - K_{sp}\delta X(s) - G_y(s)\delta Y(s) \tag{11}$$

where $\delta X(s)$ and $\delta Y(s)$ represent any lumped additive uncertainty associated with modeling error and sensor noise. Taking $R(s) = 0$ and letting $D_m(s)$ represent both plant uncertainties and noise disturbances, the equation may be rewritten as

$$U(s) = [I + K_{sp}\Phi B + G_y(s)C\Phi B]^{-1} D_m(s) \tag{12}$$

illustrating that disturbance rejection at the input corresponds to selecting the regulator weights such that

$$\underline{\sigma}\,[K_{sp}\Phi B + G_y(s)C\Phi B] \gg 1 \tag{13}$$

over the frequencies where $D_m(s)$ has the majority of its energy. It can be seen from Fig. 2 that the transfer function in Eq. (13) results from breaking the loop at the physical point 1 denoted by XX and synthesizing the relation from $U'(s)$ to $U''(s)$ with $R(s) = 0$.

Estimator Design

A Kalman filter may be used to realize the aforementioned full state feedback controller since all plant states will not be measurable in general. With the LQG method, sensor noise can be rejected from the error equation[8] by satisfying

$$\bar{\sigma}[G(s)K(s)] \ll 1 \tag{14}$$

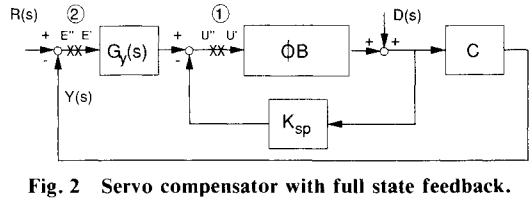

Fig. 2 Servo compensator with full state feedback.

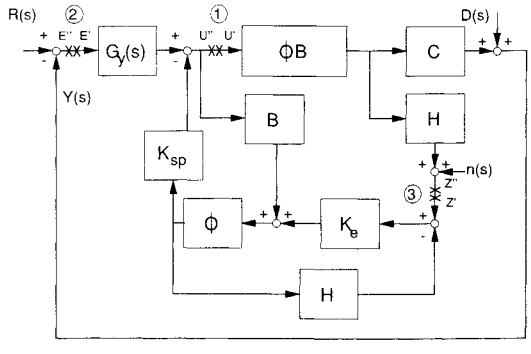

Fig. 3 Servo compensator with Kalman filter.

from Fig. 1. Employing a similar argument here and breaking the loop at the XX at physical point 3 in Fig. 3 gives

$$Z''(s) = -H\Phi B[I + G_y(s)C\Phi B]^{-1}K_{sp}\{I + \Phi K_e H + \Phi B \times [I + G_y(s)C\Phi B]^{-1}K_{sp}\}^{-1}\Phi K_e Z'(s) \quad (15)$$

which should be sufficient to describe the effect of sensor noise on $E(s)$. However, from Fig. 3 the transfer function from $\eta(s)$ to $E(s)$ with $R(s) = 0$ is

$$E(s) = C\Phi B[I + G_y(s)C\Phi B]^{-1}K_{sp}\{I + \Phi K_e H + \Phi \times (B + K_e H\Phi B)[I + G_y(s)C\Phi B]^{-1}K_{sp}\}^{-1}\Phi K_e \eta(s) \quad (16)$$

which is different from Eq. (15). Moreover, if C is identical to H as in many applications, Eq. (16) includes an additional term in the denominator that invalidates the use of Eq. (15) for Eq. (16). Consequently, Eq. (16) must be used directly by employing the standard analysis with singular values as a worst-case measure. The impact of sensor noise on the error can be minimized by making

$$\sigma(C\Phi B[I + G_y(s)C\Phi B]^{-1}K_{sp}\{I + \Phi K_e H + \Phi \times (B + K_e H\Phi B)[I + G_y(s)C\Phi B]^{-1}K_{sp}\}^{-1}\Phi K_e) \ll 1 \quad (17)$$

over frequencies where $\eta(s)$ has its energy. If the designer is unwary and uses Eq. (15) in a singular value analysis, the resulting filter will not possess the expected noise rejection properties.

The estimator design may be approached by selecting some nominal process noise intensity for Q_p (typically BB^T) and choosing $R_s = p\Gamma$, where p is a scalar parameter. The tuning parameter p can be increased or decreased such that the resulting Kalman gain (K_e) satisfies Eq. (17).

Loop Transfer Recovery

To determine the impact of the estimator on robustness, the estimator equation may be written from Fig. 3 with the loop broken at the XX at point 1 as

$$\hat{X}(s) = \Phi[BU''(s) + K_e H\Phi BU'(s)] - \Phi K_e H\hat{X}(s) \quad (18)$$

where $\hat{X}$ represents the state estimate. Rearranging terms and applying an identity gives

$$\hat{X}(s) = \Phi[B(H\Phi B)^{-1} - K_e(I + H\Phi K_e)^{-1}]H\Phi BU''(s) + \Phi K_e(I + H\Phi K_e)^{-1}H\Phi BU'(s) \quad (19)$$

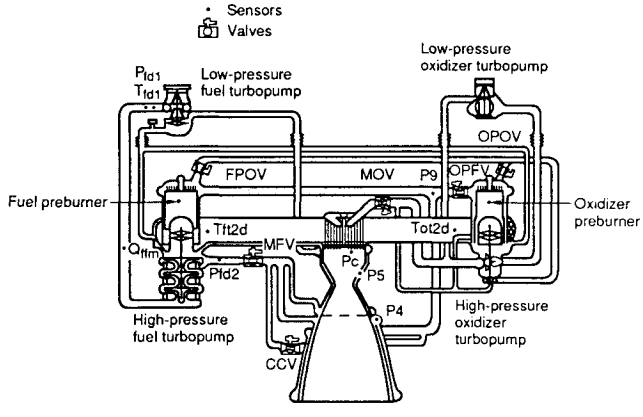

Fig. 4 Space Shuttle main engine propellant flow schematic modified by addition of the OPFV.

from which it follows that

$$B(H\Phi B)^{-1} = K_e(I + H\Phi K_e)^{-1} \quad (20)$$

will remove the estimator from the loop as in the case of standard LQG/LTR.[8]

Command following properties for the servo compensator are invariant to the introduction of the state estimator. This may be seen by rewriting the estimator equation after breaking the loop at the XX designated by point 2 in Fig. 3 as

$$s\hat{X}(s) = A\hat{X}(s) + BU(s) + K_e[Z(s) - H\hat{X}(s)] \quad (21)$$

which simplifies by substituting for $Z(s)$ and collecting like terms to yield

$$\hat{X}(s) = (\Phi^{-1} + K_e H)^{-1}(I + K_e H\Phi)BU(s) \quad (22)$$

The transfer function from $E'(s)$ to $E''(s)$ can now be written as

$$E''(s) = -C\Phi B(I + K_{sp}\Phi B)^{-1}G_y(s)E'(s) \quad (23)$$

which is identical to the full state feedback case. One of the strengths of the servo compensator approach is that the estimator dynamics do not degrade the steady-state command following performance designed into the compensator using Eq. (9).

Loop transfer recovery encounters difficulties if the realization is not invertible and minimum phase. However, these problems can be avoided with the servo compensator since H may be selected independently of C. The control objective determines C, and the available instrumentation constrains H. That is, for a given objective $\{A, B, C\}$ may not be minimum phase and/or invertible. However, H may be selected independently of the control objective based on the available measurements such that the requirements for LTR are satisfied. Additionally, in an environment where a number of control strategies (via the C matrix) may be used by reconfiguring the controller, a sensor set (H) that is invariant simplifies the overall compensator design since the nominal estimator portion of the design is performed only once.

Design Example

This paper develops a design method suited to the purpose of controller synthesis for an intelligent control system. The controller must perform over all power levels during main stage operation, provide command following with set point control, be multi-objective, perform over a variety of engine builds based on a nominal model, and be insensitive to component wear during operation. These five requirements cover the range of abilities for a controller in a reusable rocket engine intelligent control system (ICS).[1] The focus of the present design is for main stage operation defined from start plus 5 s to shutdown. Any time less than start plus 5 s is considered to be the startup. Control of the startup transients could improve the durability of the engine.[9] However, the approach developed here cannot be used directly since the dynamics during this period are not well understood, making the synthesis of appropriate $\{A, B, C\}$ difficult.

Space Shuttle Main Engine

The Space Shuttle main engine (SSME) is the first large reusable rocket engine using a staged combustion cycle with two high-pressure turbopumps (oxygen and hydrogen) fed by two low-pressure turbopumps. Figure 4 provides a propellant flow schematic of an SSME modified by the presence of an additional actuator. The SSME contains five actuators: the fuel preburner oxidizer valve (FPOV), 2) the oxidizer preburner oxidizer valve (OPOV), 3) the main oxidizer valve (MOV), 4) the main fuel valve (MFV), and 5) the coolant control valve (CCV). The original control system for the SSME uses propor-

tional-integral (PI) control via the OPOV to minimize the chamber pressure P_c error for thrust control and PI control via the FPOV to minimize the mixture ratio error. An additional valve called the oxidizer preburner fuel valve (OPFV) is added as shown in Fig. 4 to give additional control authority over the temperatures in the high-pressure turbines. The location of all control valves with respect to the turbomachinery and combustion chamber can be seen in Fig. 4. The engine is fully throtteable during main stage from 65 to 109% rated power with a rate limit on thrust commands of 10% power/s.

The proposed control design is targeted for demonstration on the Technology Test Bed at Marshall Space Flight Center, where a large number of sensors are available for feedback. For this study, 10 measurements were selected with locations on the engine as shown in Fig. 4. P_{fd1} and T_{fd1} are the discharge pressure and temperature of the low-pressure fuel turbopump, respectively; Q_{ffm} is the volumetric flow into the high-pressure fuel turbopump; T_{ft2d} and T_{ot2d} are the discharge temperatures of the high-pressure fuel and lox turbines, respectively; P_c is the pressure in the main combustion chamber; P_4 and P_5 are the pressures in the nozzle and main combustion chamber cooling jackets, respectively; P_9 is the pressure of fuel supply to the preburners; and P_{fd2} is the discharge pressure from the high-pressure fuel turbopump.

A simplified nonlinear simulation of the engine in Matrix$_x$ System Build is used for the purpose of state space model generation, control design, and analysis. The nonlinear engine model contains 39 states based primarily on flow continuity equations. Hydrogen and oxygen properties are contained in lookup tables as well as hydrogen combustion properties for use in the preburners and main combustion chamber. The additional actuator (OPFV) is modeled after the OPOV, with second-order dynamics and backlash and stiction. Each of the six actuators is modeled using 4 states, for a total of 63 states in the complete nonlinear simulation. Linear perturbation models are generated at the 65, 80, and 100% power levels without actuator dynamics for the purpose of control design. Figure 5 shows the Bode plot from the OPOV to P_c for the three power levels spanning main stage operation with each response scaled by the steady-state pressure. Recall that the

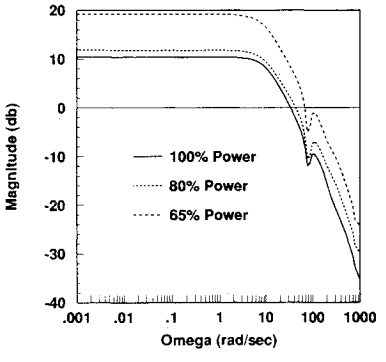

Fig. 5 Frequency response from the OPOV to P_c.

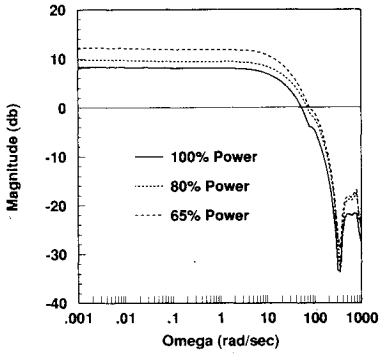

Fig. 6 Frequency response from the FPOV to the mixture ratio.

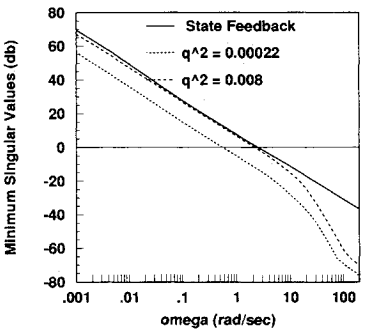

Fig. 7 Minimum singular values of closed-loop system with loop broken at point 1.

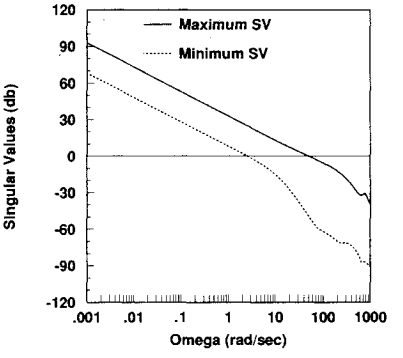

Fig. 8 Singular values of closed-loop system with loop broken at point 2.

OPOV controls thrust in the original SSME controller. The magnitude response shows very little difference between the three models over the entire frequency range, with the exception of the 65% power model, which has a slightly higher gain. Figure 6 shows the Bode plot from the FPOV to mixture ratio (MR) with each response scaled by nominal mixture ratio (6.011). Good agreement between the three models for the FPOV response (FPOV has the most influence on mixture ratio) allows one to conclude that gain scheduling on power over main stage is not necessary. This greatly simplifies the control design. For this study a design model at 100% rated power was used, since most of the time used for a typical SSME mission is spent at full power. (System matrices for the design examples are not provided due to the high order. However, the interested reader may contact the author to obtain the matrices in ASCII format on a floppy disk.)

Compensator Design

Since the rocket engine is open loop stable, the primary purpose of the controller is to allow engine throttling while maintaining the temperature in the main combustion chamber near the design point. Thrust is not a measurable quantity, but controlling P_c is sufficient to regulate thrust. The main combustion chamber temperature can be controlled by MR for any given level of thrust. However, MR is not measurable and must be estimated using P_{fd1}, T_{fd1}, P_c, and Q_{ffm}. The high-pressure turbine discharge temperatures (T_{ft2d} and T_{ot2d}) are controlled to minimize temperature excursions during transients that cause turbine blade fatigue. An additional benefit of controlling turbine temperatures can be illustrated by the following example. As the engine operates, turbine efficiency decreases resulting in higher turbine discharge temperatures to maintain thrust requirements. A large decrease in turbine efficiency can lead to temperature redlines. By controlling both thrust and turbine temperatures, the controller is able to trade off increasing turbine temperatures with decreasing thrust, thereby avoiding an engine cutoff.[10] For the present example, the controlled quantities are given by $y = [P_c\ \mathrm{MR}\ T_{ft2d}\ T_{ot2d}]^T$.

The first step in the design is the synthesis of the controller gains using regulator theory. In particular, the diagonal matrices $Q \in \Re^{r \times r}$ and $R \in \Re^{m \times m}$ must be chosen to satisfy Eqs. (9) and (13) over a specified frequency range. Thrust rates are limited on the SSME in the frequency domain by choosing Q and R such that Eq. (9) is satisfied up to 1.5 rad/s. Additionally, Eq. (13) must be satisfied over as broad a range as possible for robustness. The results of the full state feedback servo design are summarized in Figs. 7 and 8. The solid line in Fig. 7 provides a measure of the robustness in the controller with full state feedback, and Fig. 8 shows that command following constraints are met for the specified frequency range by the minimum singular value of Eq. (9). Analysis of loop shapes using singular values can be performed only after scaling of the physical quantities at the input and output of the transfer function has been performed to allow relative comparisons.

The selection $z = [P_5\ P_{fd2}\ T_{fl2d}\ T_{ot2d}\ P_4\ P_9]^T$ for state reconstruction results in a minimum phase and invertible realization $\{A, B, H\}$. The objective of the nominal design is to choose $Q_p = q^2 BVB^T$ and $R_s = p\Gamma$ such that Eq. (17) is satisfied over all frequencies. A nominal design using $q^2 = 0.00022$ and $p = 5. \times 10^6$ gave the singular value plots for sensor noise rejection shown in Fig. 9. However, Fig. 7 shows how the introduction of the estimator degrades the robustness of the controller by lowering the minimum singular value of Eq. (13). LTR can be performed by increasing q in the estimator design to recover the robustness inherent in the full state feedback compensator as shown in Fig. 7 with $q^2 = 0.008$. Robustness to uncertainty reflected at the input is costly as demonstrated by the loss in sensor noise rejection in Fig. 9. In general, LTR for the servo compensator will degrade the sensor noise rejection capacity of the Kalman filter. A balance between robustness and sensor noise rejection must be reached based on the anticipated operating environment.

Reduction of the compensator must be performed if the controller is to be considered practical due to the high order (40) and the stiffness of the estimator (the model has a number of very fast modes). Anderson and Liu[11] summarize a variety of methods, including the balanced realization technique used here. Controller reduction for the servo compensator consists of reducing the order of the stabilizing inner loop containing the Kalman filter and the state feedback gains shown in Fig. 3. For the rocket engine this approach is quite effective, since the engine is initially open loop stable and very little compensation is required to dampen the feedforward term. The servo compensator was reduced from 40 to 7 states without any loss of performance or robustness.

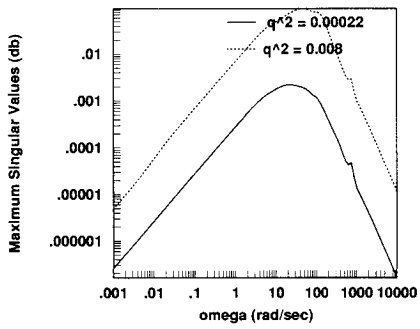

Fig. 9 Maximum singular values for sensor noise rejection.

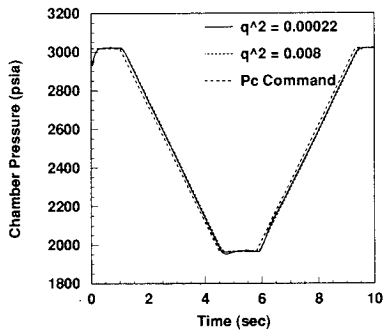

Fig. 10 Servo-compensator control of P_c through Max Q maneuver.

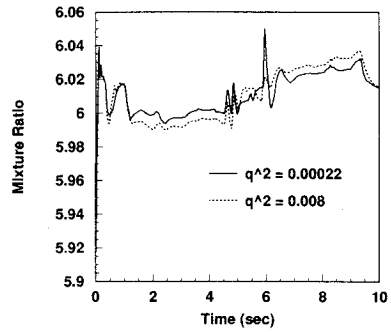

Fig. 11 Servo-compensator control of MR through Max Q maneuver.

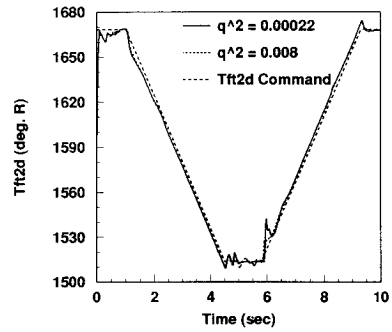

Fig. 12 Servo-compensator control of T_{fl2d} through Max Q maneuver.

Simulation Results

The reduced servo compensator was evaluated on the nonlinear simulation, including actuator dynamics by performing the Max Q maneuver. Max Q is a downthrust from full power to minimum power for a number of seconds until an upthrust command is given to return to full power. To gain a better appreciation for LTR, a comparison was made between the two controller designs without measurement noise and is shown in Figs. 10–13. Excellent control of chamber pressure is achieved throughout Max Q for both designs as shown in Fig. 10. A mixture ratio command of 6.011 is given for both controllers shown in Fig. 11. Although the nominal controller achieves slightly tighter control than the controller with loop recovery, a spike in MR at 6 s demonstrates the importance of robustness to unmodeled dynamics. Recall that the design is performed using a 100% model and the spike occurred at the 65% operating point, indicating that a certain amount of robustness is required for the 100% design to perform over all power levels. Turbine temperature control is shown in Figs. 12 and 13. Excellent command following is obtained for the given temperature profiles. The profiles shown are similar to the uncontrolled temperature responses when using the original SSME controller without the OPFV.[10] For this case the OPFV moved very little, whereas the OPOV, FPOV, and CCV follow trajectories similar to the original SSME controller. Alternate command profiles may be given for the turbine temperatures, resulting in a more active OPFV. However, the temperature commands must be consistent with the thrust requirements; otherwise, engine performance may be compromised. Profiles can be selected to minimize turbine fatigue while allowing the required thrust from the engine.

The impact of LTR on sensor noise rejection is demonstrated in Figs. 14 and 15 using a zero mean Gaussian noise generator. The mixture ratio and the discharge temperature of

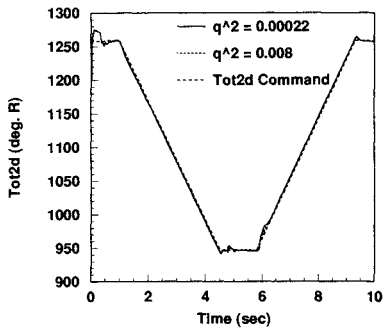

Fig. 13 Servo-compensator control of T_{ot2d} through Max Q maneuver.

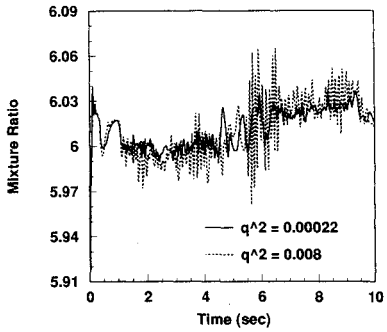

Fig. 14 Servo-compensator control of MR with sensor noise.

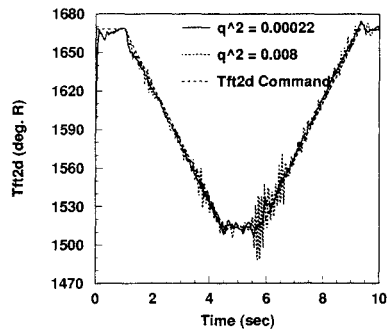

Fig. 15 Servo-compensator control of T_{ft2d} with sensor noise.

Table 1 Eigenvalues of servo compensators

Nominal controller	LTR controller
0.000	0.000
0.000	0.000
0.000	0.000
0.000	0.000
−0.0136	−0.0156
−33.47	−36.34
−65.77	−74.00

the high-pressure fuel turbine are very sensitive to sensor noise, as shown in Figs. 14 and 15, respectively. The nominal controller with a greater degree of sensor noise rejection (Fig. 9) outperforms the controller with improved robustness in terms of noise suppression. It might appear by inspection of the plots that the LTR controller must have a much higher bandwidth than the nominal controller. However, Table 1 shows that eigenvalues for the two controllers are on the same order of magnitude.

Conclusions

A frequency-domain design method using singular value inequalities is developed for the servo compensator, which is one of the fundamental components of an ICS for a reusable rocket engine. Loop transfer recovery is used to recover the required degree of robustness to uncertainty reflected at the plant input to allow for engine component wear and variations in engine builds. Loop transfer recovery suffers from several limitations. This paper shows that these limitations can be circumvented if the commands are not used for state reconstruction and a number of sensors are available for feedback, as on the SSME for the selection of a square, minimum phase, and invertible realization.

In addition, this paper demonstrates the applicability of the method to control of the SSME. In particular, a simplified nonlinear model of the engine is given based on a linear perturbation design model at 100% power. The linear design is shown to hold over the entire operating envelope during main stage. The example demonstrates the tradeoff between robustness and sensor noise rejection in the servo compensator. A certain degree of robustness is required in all designs, but the difficulty lies in finding the correct balance for each application by adjusting a single scalar parameter.

Acknowledgments

The author thanks Duane Mattern for the numerous technical discussions and helpful insights; Bob Agular at Rocketdyne for his assistance with the simplified nonlinear dynamic model of the rocket engine; and Carl Lorenzo and Walter Merrill for the opportunity to perform this work.

References

[1]Lorenzo, C. F., and Merrill, W., "An Intelligent Control System for Rocket Engines: Need, Vision and Issues," *IEEE Control Systems Magazine,* Vol. 11, No. 1, Jan. 1991, pp. 42-46.

[2]Davison, E.J., and Goldenberg, A., "Robust Control of a General Servomechanism Problem: The Servo Compensator," *Automatica,* Vol. 11, No. 5, 1975, pp. 461-471.

[3]Athans, M., "On the Design of PID Controllers Using Optimal Linear Regulator Theory," *Automatica,* Vol. 7, No. 5, 1971, pp. 643-647.

[4]Davison, E. J., "Multivariable Tuning Regulators: The Feedforward and Robust Control of a General Servomechanism Problem," *IEEE Transactions on Automatic Control,* Vol. AC-21, No. 1, Feb. 1976, pp. 35-47.

[5]Wang S., and Munro, N., "An Optimal Design Approach for the Robust Controller Problem," *International Journal of Control,* Vol. 38, No. 1, 1983, pp. 61-85.

[6]Doyle, J. C., and Stein, G., "Multivariable Feedback Design: Concepts for a Classical/Modern Synthesis," *IEEE Transactions on Automatic Control,* Vol. AC-26, No. 1, Feb. 1981, pp. 4-16.

[7]Freudenberg, J. S, Looze, D. P., and Cruz, J. B., "Robustness Analysis Using Singular Value Sensitivities," *International Journal of Control,* Vol. 35, No. 1, 1982, pp. 95-116.

[8]Ridgely, D. B., and Banda, S. S., "Introduction to Robust Multivariable Control," AFWAL-TR-85-3102, U.S. Air Force Flight Dynamics Lab., Wright-Patterson AFB, OH, Sept. 1985.

[9]Musgrave, J. L., "Advanced Control Modes for the Space Shuttle Main Engine," *Proceedings of the Conference on Advanced Earth-to-Orbit Propulsion Technology,* NASA CP-3092, Vol. 1, 1990, pp. 534-545.

[10]Lorenzo, C. F., and Musgrave, J. L., "Overview of Rocket Engine Control," *Proceedings of the Ninth Symposia on Space Nuclear Power Systems,* (Albuquerque, NM), Institute for Space Nuclear Power Studies, Jan. 1992.

[11]Anderson, B. D. O., and Liu, Y., "Controller Reduction: Concepts and Approaches," *IEEE Transactions on Automatic Control,* Vol. 34, No. 8, Aug. 1989, pp. 802-811.